

Robert F. Kirsch · Robert E. Kearney

## Identification of time-varying stiffness dynamics of the human ankle joint during an imposed movement

Received: 18 March 1996 / Accepted: 4 September 1996

**Abstract** The time-varying stiffness dynamics of the human ankle joint were identified during a large stretch imposed upon the active triceps surae muscles. Small stochastic position perturbations were superimposed upon many repetitions of the larger movement and an ensemble time-varying identification technique was then used to characterize the relationship between the small perturbation and the torque it evoked at each sample in time throughout the movement. This technique was found to provide an excellent description of the ankle stiffness dynamics throughout this movement, with the identified stiffness impulse response functions accounting for more than 80% of the torque variance at all times. The average low-frequency stiffness values ( $K_{low}$ ) derived from the stiffness impulse responses at each sample in time are believed to reflect primarily the instantaneous elastic properties of active crossbridges. These properties, which reflect the contractile state of the muscles more directly than force or torque measurements, have not been obtained previously from an intact muscle-joint system. We found that stiffness actually increased during the later portion of the large imposed stretch, indicating the triceps surae muscles did not yield significantly, and that the post-stretch steady-state stiffness level was approximately 60% higher than prior to the stretch. Reflex activity evoked by the large stretch did not produce a detectable change in  $K_{low}$ , even though this activity did produce a clear twitch-like response in joint torque beginning approximately 60 ms following stretch onset. A second-order mechanical model was found to provide an adequate characterization of stiffness dynamics for steady-state periods before and well after the imposed movement, but it could not adequately describe the observed changes in stiffness dynamics during the movement it-

self. However, the variation of model parameters indicated that the torque evoked by the stochastic displacement was predominantly elastic in nature. The stiffness behavior during stretch observed here for the intact human ankle joint is largely consistent with previous studies performed in isolated muscle preparations.

**Key words** Joint stiffness · Ankle joint · System identification · Triceps surae · Time-varying · Stretch reflex

### Introduction

Joint stiffness, the dynamic relation between the position of a joint and the torque acting about it, is an important property in the control of posture and movement. It determines the resistance generated in response to an external perturbation and can be modulated over a substantial range by changes in neural activation. Because of these properties, it has been proposed that the nervous system modulates muscle (Nichols and Houk 1976; Hoffer and Andreassen 1981), joint (Feldman 1966, 1974; Crago et al. 1976; Carter et al. 1990; Kirsch and Rymer 1992) or endpoint (Hogan 1985b) stiffness to compensate for external perturbations and/or to initiate voluntary movements. Furthermore, stiffness control has been investigated for use with electrically stimulated muscle (Crago et al. 1990, 1991; Lan et al. 1991) and has been implemented for robotic manipulators (Salisbury 1980; Hogan 1985a, 1987).

Stiffness has been studied during postural, quasi-static conditions using a variety of approaches, both in reduced animal muscle preparations and for intact human joints. These studies have shown that stiffness varies with mean joint position (Weiss et al. 1986a,b), muscle activation level (Hunter and Kearney 1982; Cannon and Zahalak 1982; Weiss et al. 1988; Kirsch et al. 1994), and perturbation amplitude (Kearney and Hunter 1982; Kirsch et al. 1994). These steady-state properties are relevant for static postural conditions but provide no information

R.F. Kirsch · R.E. Kearney  
Department of Biomedical Engineering, McGill University,  
Montréal, Québec, Canada

R.F. Kirsch (✉)  
MetroHealth Medical Center, Rehabilitation Engineering Center,  
Hamann 640, 2500 MetroHealth Drive, Cleveland,  
OH 44109-1998, USA

about joint stiffness when muscle activation and/or muscle length change, as is the case in many everyday tasks.

Several techniques have recently been developed for characterizing dynamic systems during nonstationary conditions. An earlier report from this laboratory (MacNeil et al. 1992) used an ensemble system identification method in conjunction with a small imposed stochastic displacement to describe variations in human ankle joint stiffness when subjects voluntarily changed their isometric contraction from one level to another. Bennett et al. (1992) examined the stiffness of the human elbow joint during unconstrained cyclic movements using a related ensemble technique together with the small force perturbation provided by an air-jet apparatus. More recently, Bennett (1993a,b) has examined reflex modulation of joint stiffness during rapid elbow joint movements using sinusoidal position perturbations superimposed upon a nominal joint trajectory. Elbow joint stiffness modulation has also been examined during both discrete and oscillatory voluntary movements within the context of the equilibrium point hypothesis (Latash and Gottlieb 1991a,b; Latash 1992) using slowly varying external loads and the inherent variability of subjects' reaction times. Finally, Lacquaniti et al. (1993) examined joint and endpoint stiffness during a multi-joint ball catching task, again using an ensemble identification technique; in this case, a force perturbation was applied to the upper arm and was transmitted to the elbow and wrist joints via inertial coupling.

In the current study, we have examined a behavior where time-varying ankle joint stiffness was produced by an externally applied stretch of the triceps surae muscles, rather than by changes in neural activation as in the reports cited above. Similar stretches have been widely used in the past to study intrinsic muscle properties and reflex excitability, both in isolated cat muscle (Joyce et al. 1969; Nichols and Houk 1976; Hoffer and Andreasen 1981; Kirsch et al. 1994) and at human joints (Allum and Mauritz 1984; Carter et al. 1990; Toft et al. 1991). Such studies have revealed "yielding", short-range stiffness, and other discontinuities in the force or torque responses which suggest significant changes in muscle and joint stiffness. A time-varying system identification procedure developed in our laboratory (Kearney et al. 1991; MacNeil et al. 1992) has been used to obtain estimates of the full dynamic stiffness of the ankle joint at each time sample throughout a large imposed stretch, in addition to simply measuring the net joint torque response to the stretch. Briefly, we found that the imposed stretch did not produce the decline in instantaneous joint stiffness expected during "yielding", but rather stiffness *increased* throughout most of the stretch. Stretch-evoked reflex activity produced a twitch-like increase in joint torque, but no obvious modulation of joint stiffness was detected during the same interval. A second-order mechanical model provided an accurate description of joint stiffness during steady-state conditions, but its performance deteriorated significantly during the imposed stretch. The variation of model parameters indicated that the torque

evoked by the stochastic displacement was primarily elastic in nature.

Portions of this work have appeared previously (Kirsch and Kearney 1991, 1993a).

---

## Materials and methods

The experimental and analytical techniques used in this study are virtually identical to those used previously to examine ankle joint stiffness properties during a different task (MacNeil et al. 1992) and to study time-varying electromyographic stretch reflex properties (Kirsch et al. 1993; Kirsch and Kearney 1993b); indeed, the data used here were obtained from the same experiments described in Kirsch and Kearney (1993b). These techniques are described fully in these papers and elsewhere (Kearney et al. 1991), and thus will be described only briefly below.

### Subjects and apparatus

Five human subjects, aged 22–43 years, with no known history of neuromuscular disease were tested. The experiments performed here received prior approval from the ethics committee at McGill University and conformed to the standards of the 1964 Declaration of Helsinki. Subjects provided informed consent prior to each experiment. Each subject was placed in a supine position on an experimental table with their left foot attached to a high-performance hydraulic actuator through a rigid, low-inertia fiberglass boot. Straps were applied to the hip and just above the knee (which was maintained in a slightly flexed position by a firm support) to restrict movement to the ankle joint. An oscilloscope mounted above the subject displayed a visual torque target and a torque feedback signal, lowpass filtered at 5 Hz to reduce the perturbation-evoked component.

### Signal measurement and acquisition

Signals proportional to ankle torque and angular position were provided by transducers built into the apparatus, and electromyograms (EMG) from triceps surae (TS) and tibialis anterior (TA) were obtained from surface electrodes as previously described (Kirsch et al. 1993). No attempt was made to obtain independent EMGs from the different muscles of the triceps surae group. All signals were filtered at 400 Hz by eight pole lowpass Bessel filters (Frequency Devices 902LPF) prior to sampling at 2 kHz. The D/A converter providing the "ramp" command to the actuator (see below) was also sampled to facilitate trial alignment.

### Displacement perturbations

The hydraulic actuator, configured as a rotary position servo, was used to apply a rapid "ramp" movement onto the ankle joint in the dorsiflexion direction (i.e., a stretch of the TS), upon which a small stochastic displacement was superimposed. Note that the "ramp" perturbation was actually a modified constant-velocity movement, with sharp transients at the beginning and end of the ramp stretch reduced by digital smoothing of the D/A command sequence to reduce the contribution of joint inertia to the net torque response. The resulting stretch had an amplitude of 0.13 rad (7.5°), a peak velocity of 6 rad/s (344°/s), and a peak acceleration of 343 rad/s<sup>2</sup> (19 600°/s<sup>2</sup>).

The stochastic perturbation sequence used for each subject was identical to that described in a previous study (Kirsch and Kearney 1993b). Briefly, the perturbation for each subject was derived by filtering a pseudo-random binary sequence with an impulse response function corresponding to the quasi-static ankle compliance of that subject for a 15% MVC (maximum voluntary contraction) torque level; this operation produced a displacement which

was skewed to lower frequencies so that the evoked torque response exhibited a power spectrum that was approximately flat over the frequency range of interest (0–50 Hz). The resulting command sequence was truncated to a length of 7300 (36.5 s at the 200 Hz D/A update rate) and scaled to provide a displacement with range of  $\pm 0.018$  rad ( $\pm 1^\circ$ ). Note that although the same stochastic perturbation was repeatedly cycled throughout a given experiment, its timing was not synchronized to the onset of the ramp. Because the period of the stochastic sequence was much longer than the duration of the ramp, its timing relative to ramp onset proved to be random (see below).

### Experimental paradigm

Each trial was initiated from a neutral ankle position, with the subject exerting a mean plantarflexion torque equal to 15% MVC while the small stochastic perturbation was continuously applied. When the subject had matched the desired 15% MVC contraction level to within  $\pm 5\%$  (i.e., 0.75% of MVC) for three consecutive 200-ms intervals, a second D/A converter added the command for the ramp stretch, to which the subject was instructed to “not react”. Data were recorded for 600 ms in each trial, beginning 200 ms prior to the onset of the ramp; Fig. 1 shows an example of the superimposed stochastic and ramp perturbations for one trial, along with the corresponding torque and rectified TS EMG. After a minimum of 3 s, another trial could be initiated, although the actual inter-trial intervals were somewhat longer since the subject had to voluntarily re-establish the required steady torque level and could also wait longer if desired. Sets of 32 trials were recorded in sequence, with an inter-set rest period of at least 2 min. Sixteen to twenty-four sets were recorded in a given experiment, for a total of 512–768 trials.

Several additional trials were also recorded in each experiment. First, a 30-s trial with the stochastic perturbation only (i.e., no ramp stretch) and a mean torque of 15% MVC was recorded for all subjects to characterize quasi-static stiffness properties at a neutral ankle position. In two of the five subjects, additional 30-s stochastic-only trials were recorded at five equally spaced mean positions across the span of the ramp stretch. In the same two subjects, a set of 250 trials with the large stretch and superimposed stochastic perturbation were recorded as described above, but in this case the subject was instructed to remain completely relaxed. Finally, 32 trials with the ramp perturbation only were recorded at an initial 15% MVC contraction level for all five subjects.

### Analysis

#### *Trial alignment and selection*

The trial alignment and selection procedures described previously (Kirsch et al. 1993) were again used to choose the 250 “most similar” trials. All trials were first aligned to the D/A ramp command recorded at 0.5-ms intervals, then the most similar trials were selected using a mean-square error criterion between lowpass filtered (18 Hz) torque responses. This filtering reduced the component of the torque response due to the stochastic perturbation while having minimal effect on the torque response evoked by the ramp stretch, thus concentrating the selection process upon the underlying time-varying behavior rather than on the perturbation-related component (which was by design different in each trial). The position, torque, and digitally rectified EMG records were then decimated (after digital anti-alias filtering) to a final sampling rate of 250 Hz, which was more than adequate to capture stiffness dynamics for the 50-Hz bandwidth stochastic perturbation.

#### *Time-varying system identification*

An ensemble time-varying identification procedure was used to track time-varying ankle stiffness properties. A full description of

this approach and its benefits relative to other time-varying identification techniques can be found elsewhere (Kearney et al. 1991; MacNeil et al. 1992; Kirsch et al. 1993). The end result of this identification process was a set of 43-point (168-ms), two-sided impulse response functions representing ankle stiffness dynamics at 4-ms intervals throughout the imposed ramp stretch. Goodness of fit was assessed by convolving the experimentally recorded position ensemble with these identified stiffness impulse responses to obtain a predicted torque ensemble, and then computing the percentage of variance accounted for (%VAF) between the actual and predicted torque ensembles, both across time at particular instants in the time-varying behavior and across individual trials (Kirsch and Kearney 1993a).

#### *Second order model fits*

Ankle stiffness dynamics were summarized by fitting a second-order model of the form  $T(t) = K\theta(t) + B\dot{\theta}(t) + I\ddot{\theta}(t)$  (where  $T$  is ankle torque,  $\theta$  is ankle angle,  $K$  is joint elastic stiffness,  $B$  is joint viscosity and  $I$  is joint inertia) to the stiffness frequency responses obtained by Fourier transforming the stiffness impulse responses. Such a second-order model has been widely used to describe joint stiffness properties (Hunter and Kearney 1982; Kearney and Hunter 1982; Cannon and Zahalak 1982; Weiss et al. 1986a,b, 1988; Bennett 1993a). The parameters of the model were fit to the complex-valued stiffness frequency response at each sample in time using a Levenberg-Marquardt nonlinear least-squares algorithm (Optimization Toolbox for Matlab, The MathWorks). Each fit was performed over a frequency range of 8–50 Hz, the upper limit set by the highest frequency component in the stochastic perturbation and the lower limit set primarily by the length of the stiffness impulse responses; longer impulse responses would have provided finer frequency resolution, but the identification of these longer impulse responses would have required a correspondingly larger (and impractical) number of experimental trials. Moreover, the range of frequencies used in the fit was found to be more than adequate to describe dynamic behavior of the joint (see below). The goodness of fit of the second-order model was assessed by generating an ensemble of stiffness impulse responses from the second-order parameters (one for each sample in time) and following the same procedure used for the identified, nonparametric stiffness impulse responses described above.

## Results

### Responses to ramp and stochastic position perturbations

#### *Basic properties*

Figure 1 shows both single trial and ensemble average data for a single subject. The position records illustrated in Fig. 1A show the net positional variations imposed by the hydraulic actuator in one trial (the thin continuous line), as well as the two components of this net perturbation. The ensemble average position across all 250 selected trials (thick continuous line) indicates the large dorsiflexing ramp stretch (0.13 rad or  $7.5^\circ$ , 25 ms duration, peak velocity 6 rad/s) that was common to each trial, while the thin dashed trace shows the small stochastic perturbation that was unique to each trial. Also shown in Fig. 1A (as the thick dashed trace) is the ensemble standard deviation, whose constancy across time indicates that the stochastic perturbation was stationary across time in single trials. Furthermore, this ensemble standard deviation was found to be equal to the standard deviation

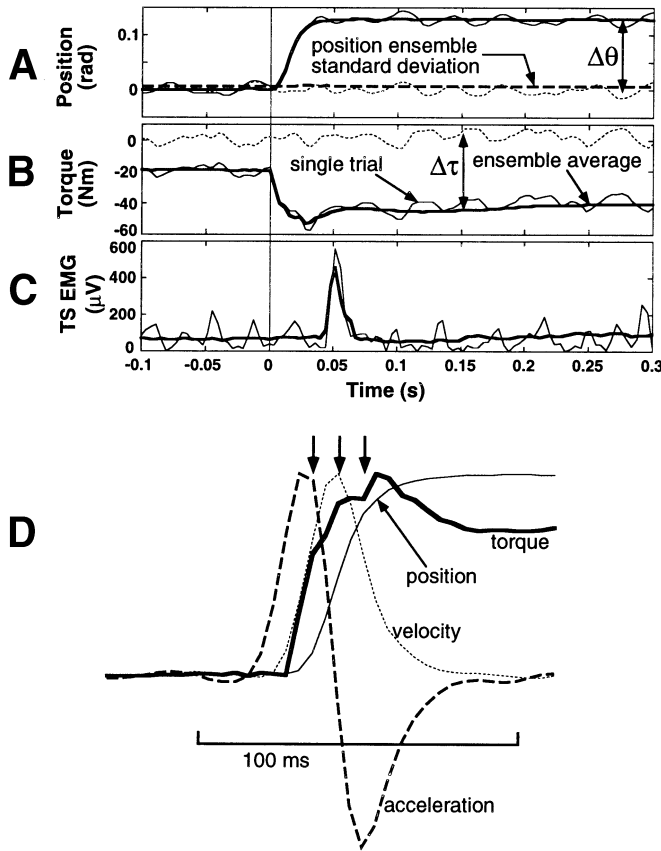


**Fig. 1A–D** A–C Single trial data records. **A** Ankle position, showing the ensemble average of the 250 selected trials (*thick trace*), the stochastic perturbation imposed in a single trial (*thin dashed trace*), and the sum of the two (*thin continuous trace*). The ensemble standard deviation is shown as the *thick dashed trace*. **B** Ankle torque, showing the ensemble average response (*thick trace*), the response to the stochastic perturbation alone (*thin dashed line*), and the sum of the two (*thin continuous solid trace*). Note that plantarflexion torque is shown increasing in the negative direction. **C** Rectified triceps surae (TS) electromyogram (EMG) responses, showing the ensemble average (*thick trace*) and a single trial response (*thin trace*). **D** Normalized joint torque, position, velocity, and acceleration records for same subject as in A–C. Velocity and acceleration were obtained from numerical differentiation of position record. *Arrows* indicate times where slope of torque response changes

of the stochastic perturbation across time in a single trial. This demonstrates that the properties of the perturbation were very similar across all trials and that the timing of the large imposed stretch was random relative to the superimposed stochastic perturbation (for a more detailed discussion see Kirsch et al. 1993).

The torque records shown in Fig. 1B indicate the responses to the ramp stretch alone (the ensemble average), the stochastic perturbation alone, and the combination of the two. The large stretch produced a rapid increase in torque that settled after an overshoot to a steady-state level approximately twice the pre-stretch value, while the stochastic position perturbation resulted in smaller, random changes in torque. The TS EMG (Fig. 1C) exhibited a large synchronous reflex response

beginning approximately 40 ms after stretch onset and smaller continuous variations evoked by the stochastic perturbation. A steady-state increase in TS EMG following the imposed stretch was also found, with the mean steady-state EMG increasing across all subjects by an average of 24.7% relative to the pre-stretch mean EMG. Although not obvious in Fig. 1, a twitch-like increase in torque was often observed (see Fig. 5) beginning approximately 60 ms following stretch onset, and was presumably associated with the synchronous reflex burst of TS EMG occurring 20 ms earlier. TA EMG records are not illustrated in Fig. 1, but we found TA activity to be negligible in all subjects. Maximum TA EMG levels were typically less than 5% of that of the TS EMG, and the time course of the TA EMG was very similar to that of the TS EMG. This suggests that the main source of the recorded TA EMG was a small degree of crosstalk from the TS group, and it is therefore highly unlikely that the ankle dorsiflexor muscles contributed to the mechanical responses described below.

Figure 1D plots the same ensemble average torque and position records as in Fig. 1A and B, but in a normalized form and using an expanded time scale. Superimposed on these records are normalized velocity and acceleration records obtained by numerically differentiating the position record. The vertical arrows indicate break points where the slope of the torque record exhibited clear changes. Note that the leftmost break point coincides with the decrease of acceleration from its peak positive level, the center break point coincides with the decrease of velocity from its peak, and the rightmost break point coincides with an increase in acceleration from its peak negative level. These features were highly repeatable across all five subjects.

#### *Effect of stochastic perturbation on torque response to ramp stretch*

The imposition of the stochastic position perturbation was found in all subjects to enhance the torque generated in response to the larger ramp stretch. The lower traces in Fig. 2 compare the torque ensemble averages obtained from two subjects using the 250 ramp+stochastic perturbation trials with those obtained from these same two subjects in the 32 ramp-only trials. For both subjects, the pre-ramp torque level produced by the subject was the same with or without the stochastic perturbation, but the imposed ramp stretch resulted in a significantly larger torque response when the stochastic perturbation was present. This behavior was found for all five subjects, and is summarized in the upper portion of Fig. 2 by the difference in the torque ensemble averages obtained with and without the stochastic perturbation. The response enhancement occurred very rapidly, reached its peak value before the onset of reflex action, and was maintained for an interval longer than voluntary reaction times.

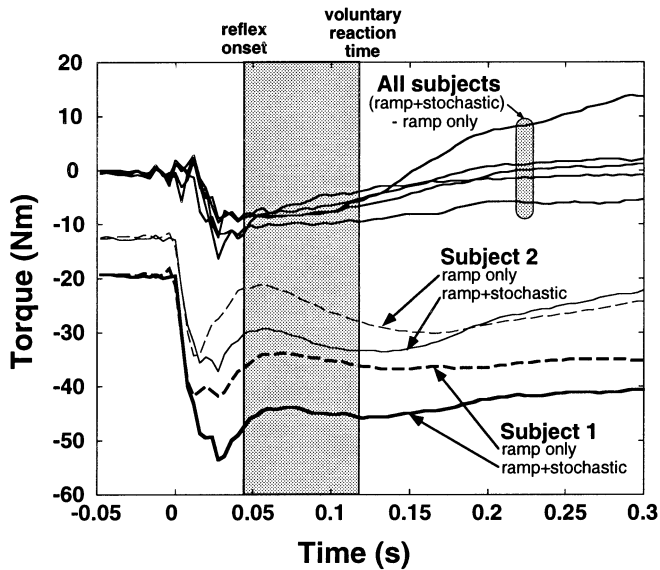


**Fig. 2** Effect of the stochastic perturbation on the torque response to the ramp stretch. The lower portion of the figure shows the responses to the ramp stretch with (*continuous traces*) and without (*dashed traces*) the stochastic perturbation superimposed, for two subjects (*thin traces and thick traces*). The upper traces show the differences between the torque responses with and without the superimposed stochastic perturbation for all five subjects

#### Nonparametric stiffness properties

##### *Stiffness dynamics: impulse response and frequency response ensembles*

The 250 “most similar” trials remaining after the trial selection procedure were input to the ensemble time-varying identification procedure, which produced estimates of ankle joint stiffness impulse response functions at each time sample (i.e., every 4 ms) throughout the experimental trial. Representative impulse responses are shown in Fig. 3A for three times: during the pre-stretch steady state, during the middle of the imposed stretch, and during the post-stretch steady state.

Although time-varying joint stiffness dynamics are most conveniently *identified* using two-sided impulse response functions, these impulse responses are difficult to *interpret* because they are noncausal and dominated by inertial contributions. Fortunately, these impulse responses can readily be transformed to the frequency domain using the Fast Fourier Transform (FFT), and the resulting stiffness frequency responses illustrate the relevant low-frequency components of joint stiffness much more clearly. Figure 3B illustrates the magnitude portion of the ensemble of stiffness frequency responses obtained in this way for one subject. In this figure, time during the trial progresses along the “Time” axis, while the stiffness dynamics at each time are shown by individual traces along the “Frequency” axis. The pre-stretch frequency response at -100 ms shows the basic form of ankle stiffness dynamics familiar from time-invariant studies: stiffness magnitude is relatively flat at low fre-

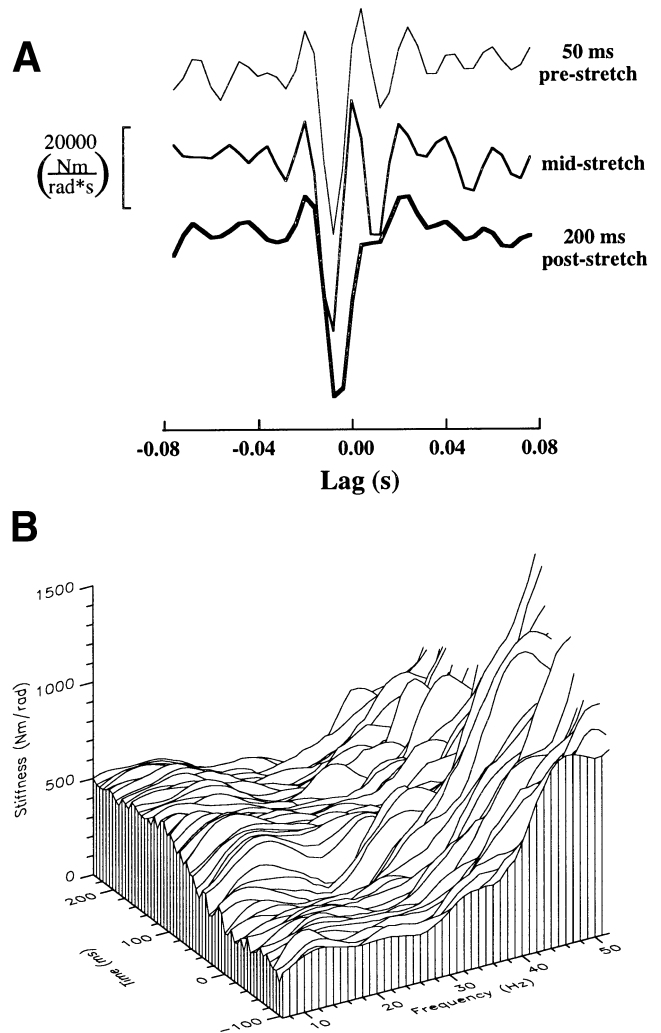


**Fig. 3A, B** Stiffness dynamics across time during the imposed stretch for one subject. **A** Stiffness impulse responses identified before, during, and following the imposed stretch. Note that impulse responses have been minimally smoothed to remove noise near the Nyquist frequency. **B** Stiffness frequency response magnitude ensemble; stretch applied at time zero and each curve represents the absolute value of the Fast Fourier transform of the stiffness impulse response identified at that time

quencies, exhibits a resonance at approximately 25–30 Hz, and thereafter increases with frequency due to the inertia of the joint. Following the imposed stretch (at time 0), stiffness magnitudes at low frequencies clearly increased, but this did not occur instantaneously and the shape of the frequency responses changed as well as the amplitude. These changes will be described in more detail below.

##### *Goodness of fit*

The ensemble of time-varying stiffness impulse responses described ankle stiffness properties throughout the imposed stretch very well, as illustrated in Fig. 4. In this figure the recorded joint torque (thin traces) is superim-

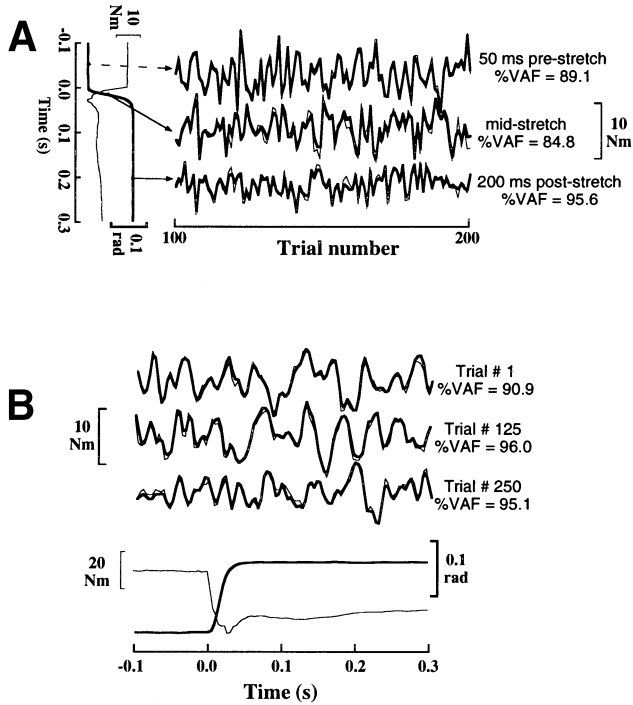


**Fig. 4A, B** Comparison of recorded torque with that predicted by time-varying stiffness impulse responses. Recorded torques (with ensemble average subtracted) are plotted with *thin lines*, predicted torques by *heavy lines*. **A** Actual and predicted torque for the three indicated times during the task, plotted across 100 trials. Note that the percentage of variance accounted for (%VAF) is computed across all 250 trials. **B** Actual and predicted torque plotted across time for single trials at the beginning, middle, and end of one experiment. Timing relative to the behavioral task is indicated by torque and position ensemble averages at the *bottom*

posed on that predicted by convolving joint position with the time-varying stiffness impulse responses (heavy traces). This comparison has been done across the ensemble of trials at three different times (Fig. 4A). The close correspondence between the actual and predicted torques indicates that the experimental and analytical techniques were successful in freezing and capturing joint dynamics at each time, even during the middle of the large imposed stretch.

A similar comparison was also carried out for individual trials. Figure 4B shows the actual and predicted torques for trials at the beginning, middle, and end of the experiment. Again, the predicted and observed torques were very similar, indicating that a single set of time-varying stiffness impulse responses described stiffness dynamics accurately throughout the entire experimental session.

#### Low-frequency stiffness

We generated an empirical indicator of stiffness variations across time by computing  $K_{low}$ , the average low-frequency stiffness, as the average value of the stiffness frequency response magnitude between 10 and 20 Hz (depicted by the shaded rectangle in the lower panel of

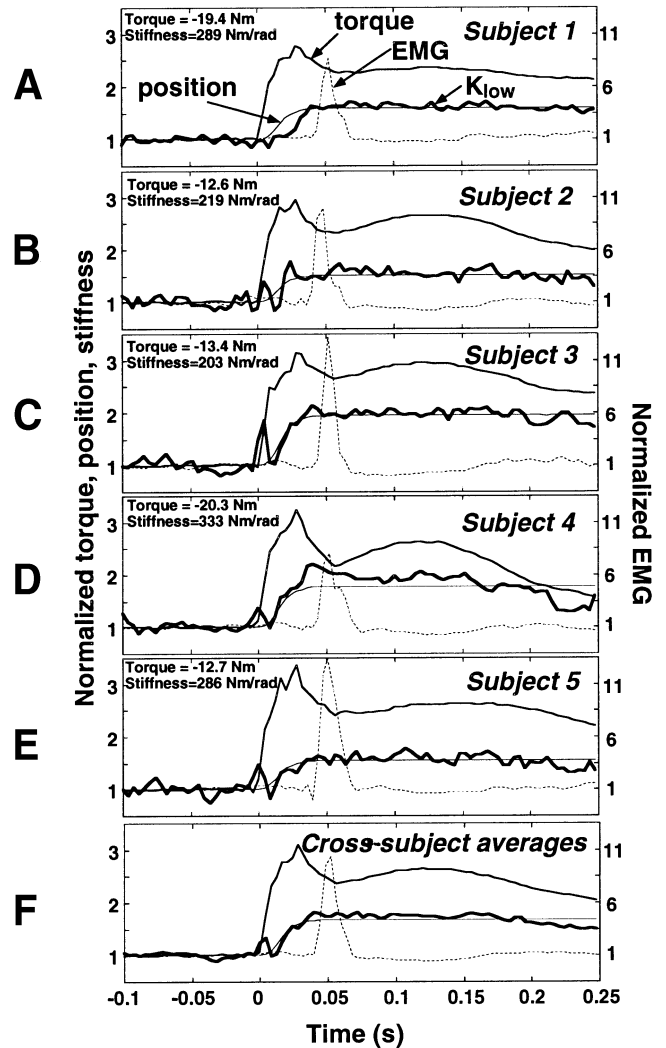


**Fig. 5A–F** A–E Normalized ensemble average position, torque, and EMG responses plotted with normalized low-frequency stiffness ( $K_{low}$ ) for all five subjects. Torque, EMG, and  $K_{low}$  are normalized to their pre-stretch average values (absolute pre-stretch torque and stiffness average values indicated in each panel); position ensemble averages are scaled to fit the range of  $K_{low}$  for each subject. Note that the EMG scale is to the *right*. **F** The average position, torque, EMG, and  $K_{low}$  taken across the responses of all five subjects in A–E

Fig. 7A) for each frequency response in the ensemble. (Note that a more detailed description of stiffness dynamics in terms of a parametric model will be given below.) Figure 5 shows  $K_{low}$  as a function of time, along with the ensemble averages of position, torque, and TS EMG, for all subjects. All quantities except position have been normalized to their average values prior to the onset of the ramp. (The average pre-stretch torque and stiffness values are indicated for each subject since the contraction level was defined as a percentage of each subject's MVC rather than an absolute level. Note that the scale for TS EMG is somewhat larger than for the other quantities and is shown to the right of each panel.)

The position ensemble averages were essentially identical for all subjects, but were scaled in each panel of

Fig. 5 to match the range of that subject's  $K_{low}$  to facilitate a comparison of their time courses. For all subjects, low-frequency stiffness was nearly constant during the steady-state intervals before and well after the stretch, but increased by 50–100% following the stretch. At the onset of the stretch, most subjects showed a transient increase in  $K_{low}$  followed by a more gradual increase to the final steady-state level. In three subjects (i.e., subjects 3–5) the time course of this gradual increase in  $K_{low}$  was very similar to that of the imposed ramp stretch, while the stiffness of the other two subjects followed a somewhat more variable trajectory to the final steady state. In all subjects, however,  $K_{low}$  increased towards its final steady-state value at the same time as the active TS muscles were being rapidly and forcibly lengthened.

The time course of  $K_{low}$  was not affected by the sizable reflex activation indicated by the large burst of TS EMG at 40–45 ms following ramp onset. This burst was highly repeatable and evoked clear twitch-like torque responses in all subjects. For all subjects, however,  $K_{low}$  reached its steady-state value prior to the onset of this reflex burst and did not increase even during the subsequent reflexive increase in joint torque.

#### Static position dependence of stiffness

The similarity in the time course of the average low-frequency stiffness,  $K_{low}$ , and that of the ramp position perturbation led us to examine the effect of static joint position on joint stiffness. For two subjects, stochastic perturbations (without the large stretch) were applied at six different mean joint positions across the range of the stretch imposed in other trials, and stiffness dynamics were estimated using quasi-static methods. The low-frequency stiffness values resulting from these trials are plotted for both subjects in Fig. 6; the zero position corresponds to the pre-stretch position in ramp stretch trials, while the 0.13 position is near the final position of the ramp. For both subjects there was little change in joint stiffness with static position over the range examined (which was near the neutral position of the joint). Moreover, the stiffness magnitudes were comparable to those obtained for the pre-stretch steady-state period of time-varying trials (compare with the pre-stretch values indicated in Fig. 5).

Parametric modeling: variations in elastic, viscous, and inertial components

#### Single-subject responses

As described in the Materials and methods, a second-order model with parameters corresponding to the elastic, viscous, and inertial properties of the ankle joint was fitted to the stiffness frequency response obtained at each time sample. Several examples of the fits obtained for one subject are shown in Fig. 7A. The change in the stiffness dynamics across time is evident in the progres-

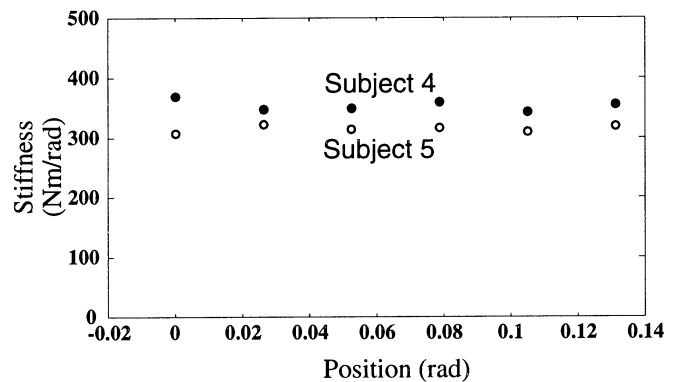


**Fig. 6** Dependence of quasi-static stiffness on mean joint position for two subjects. Time-invariant identification was used at each position; mean joint position was varied to six locations equally spaced over the range of the ramp stretch used in this study

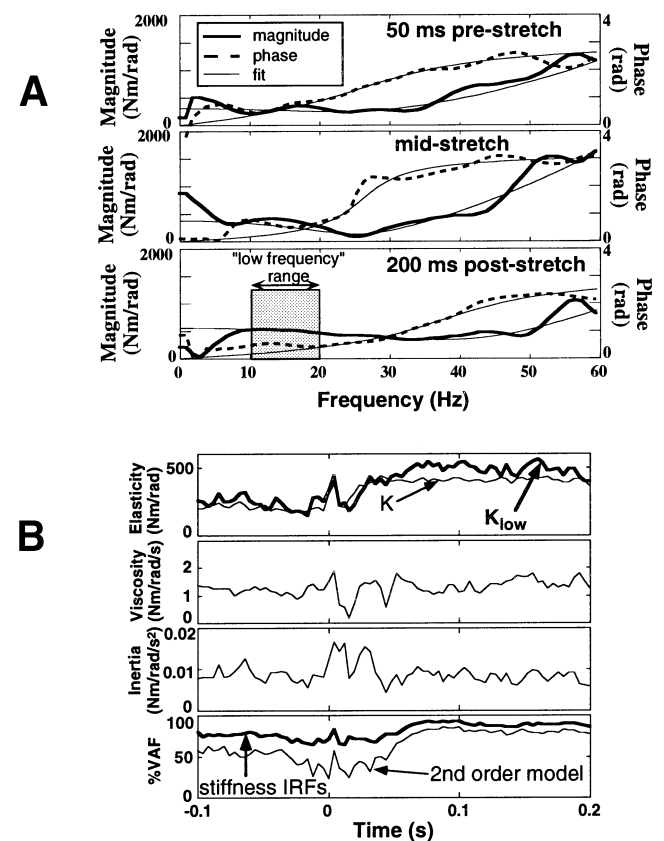


**Fig. 7A, B** Second-order modeling of time-varying ankle joint stiffness for subject 1. **A** Identified and modeled stiffness frequency responses for same times as in Fig. 4A. *Heavy continuous trace* indicates identified stiffness magnitude (scale to the left), *heavy dashed trace* indicates identified phase (scale to the right). *Thin traces* indicate responses predicted by the best-fit second-order model. *Lower panel* indicates frequency range for low-frequency stiffness average,  $K_{low}$ . **B** Parameter variations and goodness of fit for second-order model parameters (*light traces*) for subject 1.  $K_{low}$  and the %VAF of the nonparametric stiffness impulse responses are shown with *thick traces*

sive increase in the low-frequency magnitude and break frequency from the top to the bottom panel in Fig. 7A, indicating that the joint has become stiffer.

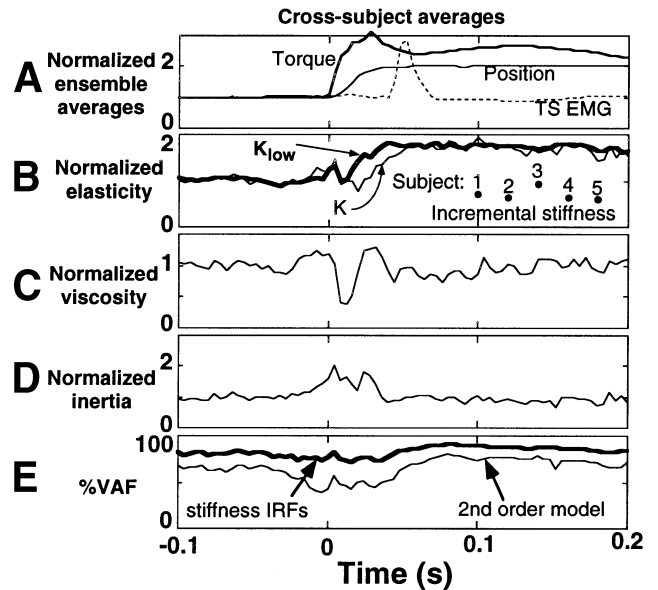
Figure 7B plots the variation of the elastic, viscous, and inertial parameters of the second-order fits for one subject as functions of time during the experimental trial. As shown in the upper panel of Fig. 7B, the variation of the elastic parameter  $K$  was similar to that of the average low frequency stiffness,  $K_{low}$ ; moreover the pre-ramp steady-state values were very similar to those obtained previously during quasi-static conditions (Hunter and Kearney 1982; Weiss et al. 1988). The pre-ramp values estimated for the viscous and inertial parameters were also similar to those found for quasi-static conditions, but both parameters changed in a complex manner during the imposed ramp stretch. The viscous parameter exhibited a transient change immediately after ramp onset, and then again at the termination of the ramp. The inertial parameter nearly doubled during the ramp stretch, even though its value would be expected to remain constant over the range of joint angles examined here.

The bottom panel of Fig. 7B compares the ability of the nonparametric stiffness impulse responses and the corresponding second-order models to predict the experimental torque responses. For all times during the trial, the stiffness impulse responses predicted the perturbation-evoked torque more accurately than the second-order model; this was most evident during the large imposed stretch, where the %VAF of the second-order model fell below 50% while that of the stiffness impulse responses remained above 80%.

#### Population averages

The single-subject results shown in Fig. 7B were typical for all subjects. The overall population behavior is illustrated in Fig. 8 as normalized parameter values; the parameters (elasticity, viscosity, and inertia) for each subject were first normalized with respect to that subject's pre-stretch average parameter values, and the resulting normalized records were then averaged across subjects. The average elastic parameter followed a course similar to that of  $K_{low}$ , except during the ramp stretch itself, when  $K_{low}$  increased more rapidly than the elastic parameter. At the same time, the viscous parameter exhibited large and complex changes, while the inertial parameter nearly doubled. These unusual variations in the second-order model parameters during the stretch were accompanied by a significant deterioration in the goodness of fit, with the model accounting for less than 50% of the torque variance on average while the nonparametric stiffness impulse responses accounted for approximately 80% of the variance during this period.

Steady-state incremental stiffness measurements for each subject are plotted in Fig. 8B for comparison with the elastic and  $K_{low}$  estimates. Incremental stiffness was computed by dividing the incremental steady-state torque response to the ramp stretch (indicated as  $\Delta\tau$  in



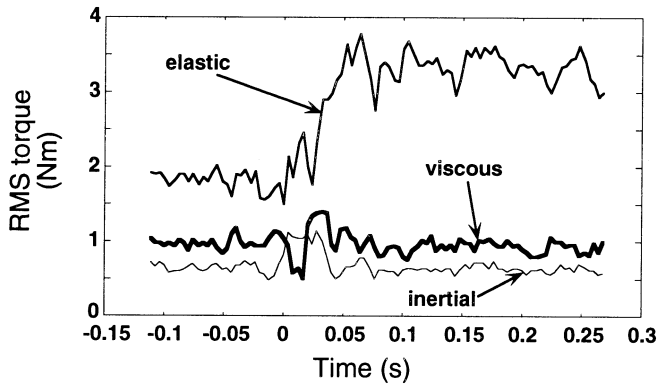
**Fig. 8A–E** Summary of parametric modeling: normalized cross-subject averages. **A** Position, torque, and EMG ensemble averages, averaged across subjects as in Fig. 5F. **B–D** Time variations of the parameters of the second-order model, averaged across subjects after being normalized with respect to their respective pre-stretch average values. **B** includes the average time variations of  $K_{low}$  across subjects (*thick trace*), as well as the average steady-state incremental stiffness for each subject (*filled circles*) for reference. **E** Average %VAF for the second-order model (*thin trace*) and nonparametric stiffness impulse responses (*thick trace*) across all five subjects

Fig. 1) by the corresponding steady-state positional change ( $\Delta\theta$  in Fig. 1). This quantity was computed for each of the 250 selected trials for each subject and then averaged across trials to obtain a single estimate for each subject; note that the standard deviation of the steady-state stiffness across trials produced error bars smaller than the plotting symbol used in Fig. 8B, indicating the similarity of the trials. For presentation purposes, the incremental stiffness was normalized by the average pre-stretch  $K_{low}$ . All five subjects showed similar relative behavior, with incremental stiffness magnitudes approximately 60–100% of the pre-stretch  $K_{low}$ .

#### Relative elastic, viscous, and inertial torque contributions

Figure 9 plots the predicted contributions of the elastic, viscous, and inertial model parameters to the torque evoked by the stochastic perturbation for subject 1. These curves were computed by taking the 250 joint position data points across the ensemble of trials at each time, numerically computing joint velocity and acceleration, taking the root-mean-square (RMS) values of position, velocity, and acceleration, and finally multiplying these RMS values by the elastic, viscous, and inertial stiffness estimates, respectively, for that time. Prior to the stretch, the elastic component was responsible, on average, for





**Fig. 9** Relative contributions of the elastic, viscous, and inertial terms of the second-order model to the evoked torque. Traces are computed as the root-mean-squared (*RMS*) value of position (elastic), velocity (viscous), or acceleration (inertial) at each time across the ensemble of 250 trials, multiplied by the appropriate parameter at that time

nearly twice the torque produced by viscous effects and approximately 3 times that produced by inertia. During the stretch, the second-order model was not accurate, but following the stretch the elastic torque component increased by almost 100% while the other two components were essentially unchanged, resulting in a clear dominance of elastic properties during this period.

#### Passive torque and stiffness components

Figure 10A examines the contributions of passive joint properties to the torque evoked by the large imposed ramp stretch. Each curve in Fig. 10A represents a different subject and was computed by dividing the torque ensemble average for the 32 ramp-only trials obtained with the subject completely relaxed (“passive”) by the corresponding ensemble average from the 32 ramp-only trials with the subject contracting to 15% MVC. Over the first 40 ms, a substantial fraction of the response is passive and due primarily to the inertia of the joint. After 50 ms post-onset, however, the response flattens out, with the “passive” response accounting for approximately 10–50% of the total response in different subjects. We had significant difficulty obtaining truly passive responses from most subjects, however, as indicated by the corresponding “passive” EMG responses illustrated in Fig. 10B. These EMG stretch responses, normalized by the peak of the active response of each subject, were significant in 4 of 5 subjects; only the subject illustrated by the heavier trace showed negligible reflex activity, and the passive torque component for this subject (heavy trace in Fig. 10A) was the smallest by far. Judging from this subject and from the other subjects prior to the onset of reflex activity, passive properties probably accounted for between 10% and 25% of the net torque response to ramp stretch.

Passive time-varying stiffness properties were also characterized in two of our five subjects by recording

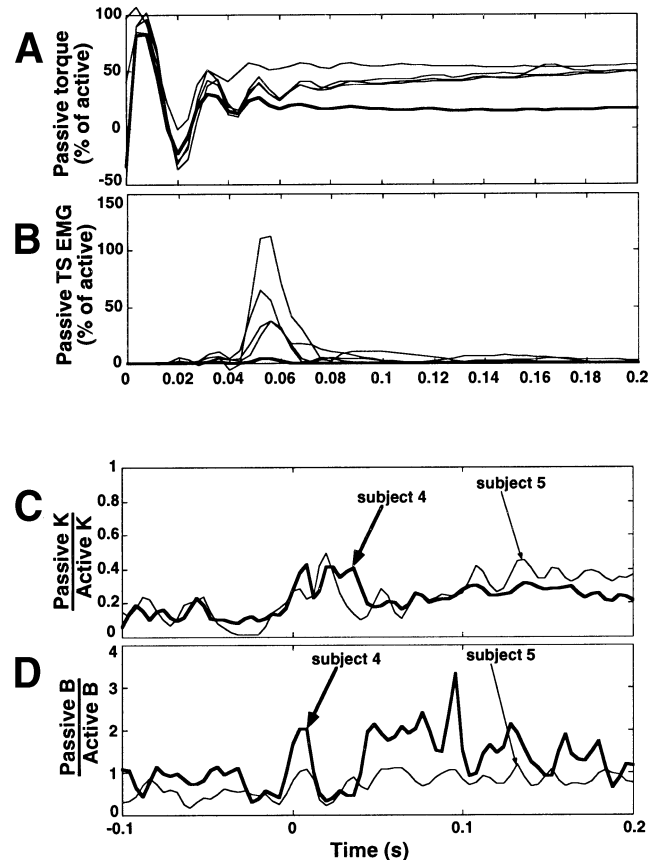


**Fig. 10A–D** Passive torque and stiffness properties. **A** Passive ensemble average torque responses divided by the corresponding active ensemble average at each time for each subject and plotted as a percentage. **B** Ensemble average EMG responses to the ramp stretch for all five subjects for “passive” conditions, normalized by their respective peak active EMG values. *Heavy traces* in **A** and **B** indicate subject 2, who exhibited the smallest reflex EMG under passive conditions. **C** Passive elastic stiffness divided by the corresponding active elastic stiffness for subjects 4 and 5. **D** Passive viscosities divided by the corresponding active viscosities for these same two subjects

250 trials with the large stretch and superimposed stochastic perturbations (i.e., identical to the main body of experimental trials), but with the subject relaxed rather than contracting at 15% MVC. A set of time-varying stiffness impulse responses was identified and second-order models were fitted to the corresponding stiffness frequencies as for the active trials. Figure 10C and D summarize these results by plotting the resulting passive elastic and viscous stiffness estimates, respectively, for both subjects, normalized with respect to the corresponding active parameters for that subject. Prior to the stretch, the passive contribution to elastic stiffness was less than 20% for both subjects, but it clearly increased as a fraction of the net stiffness following the imposed stretch, averaging 32.5% of the total stiffness for subject 4 and 24.7% for subject 5. The passive contribution to net viscous stiffness was a greater fraction of total viscosity, averaging 48.7% and 95.9% for the pre-stretch period for subjects 4 and 5, respectively, and being even

larger during the post-stretch period. It should be noted again that the post-stretch “passive” elastic and viscous stiffness values of both these subjects almost certainly contained an active component since both had significant reflex responses to the imposed stretch even while relaxed. The pre-stretch behavior indicates, however, that the passive contribution to elastic stiffness was rather small for the position tested, while passive properties produced a significant fraction of the net viscosity.

---

## Discussion

We have used an ensemble time-varying identification technique to characterize the instantaneous stiffness dynamics of the human ankle joint throughout a large, rapid stretch imposed upon the active TS muscles. The rapid stretch produced large joint torque and TS EMG responses, but excellent descriptions of instantaneous stiffness dynamics were obtained throughout the imposed movement using the torque responses evoked by a small stochastic perturbation superimposed upon the larger stretch.

Low-frequency stiffness ( $K_{low}$ ) was increased by the stretch by approximately 60% on average and reached its final steady-state value before the termination of the stretch and well before any reflex activity evoked by it. Reflex activity evoked by the large stretch produced a clear twitch-like response in joint torque beginning approximately 60 ms following stretch onset, but had no apparent effect on the instantaneous joint stiffness. A second-order mechanical model described stiffness dynamics well during the pre-stretch and post-stretch steady-state periods. However, during and immediately following the imposed stretch, the goodness of fit declined significantly and the model parameters varied in a complex and seemingly inappropriate manner. The following sections will discuss methodological issues relevant to our conclusions, possible mechanisms mediating the observed stiffness properties, and the physiological significance of the results.

### Methodological considerations

#### *Dynamics and identification of time-varying properties*

The time-varying identification technique used here was developed specifically for characterizing time-varying dynamic systems, and thus is capable of distinguishing between effects due to the stiffness dynamics themselves and the change of these dynamics across time, with a temporal resolution limited only by the sampling interval. This fine resolution is attained by using data from many similar trials rather than across time in a single trial, so it is referred to as an *ensemble* approach. A more detailed discussion of the relative advantages of this technique can be found in Kirsch et al. (1993). In the current application, this time-varying identification tech-

nique allowed us to track the rapid changes in ankle joint stiffness by an imposed stretch in a manner not previously possible in an intact system.

#### *Linearity and goodness of fit*

A *linear* time-varying identification technique was used here, even though muscle and joint stiffness properties are known to exhibit several nonlinear features. Previous quasi-static studies (Hunter and Kearney 1982; Kearney and Hunter 1982; Weiss et al. 1988; MacNeil et al. 1992) have shown ankle joint stiffness to be quite linear for small stochastic perturbations; in the present study, stiffness was linearized about the time-varying imposed ramp stretch. The resulting time-varying stiffness impulse responses were found to provide an excellent description of ankle joint dynamics, accounting for between 80% and 95% of the torque variance related to the stochastic perturbation throughout the experimental trial (Figs. 7, 8). The highest %VAFs were reached during steady-state conditions, while the slightly lower levels were observed during and immediately after the imposed stretch. The higher %VAF post-stretch relative to pre-stretch probably results from the higher stiffness observed during this period; a higher stiffness will provide larger torque variations for a fixed displacement amplitude, so the effects of fixed amplitude noise (i.e., torque components not related to the stochastic perturbation) will be reduced. The form of the stiffness impulse responses (and the stiffness frequency responses derived from them) was in general quite similar to that obtained under quasi-static conditions. Furthermore, stiffness magnitudes from the pre-stretch steady-state period obtained using the time-varying method were very similar to corresponding quasi-static stiffness estimates. Thus, the nonparametric description of stiffness dynamics afforded by the time-varying ensemble of stiffness impulse responses was very good. We therefore also have high confidence in the low-frequency stiffness values ( $K_{low}$ ) obtained from these impulse responses.

### Ankle stiffness dynamics and modeling

The nonparametric  $K_{low}$  quantity is important because it represents the static stiffness available to reject external disturbances. However, the frequency responses illustrated in Fig. 7 clearly show that the dynamic properties of the joint also changed significantly during and following the imposed stretch. The increase in stiffness magnitude at low frequencies and the shift in the natural frequency seen in these records during and following the stretch are consistent with an increase in elastic stiffness, but a more complete assessment of stiffness dynamic properties was attempted by fitting a second-order model to the stiffness frequency responses. This fitting process provided elasticity, viscosity, and inertia estimates at each point during the trial. In agreement with previous results obtained

under quasi-static conditions (Hunter and Kearney 1982; Weiss et al. 1988), we found that a second-order parametric model of ankle joint stiffness dynamics performed well during steady-state conditions, accurately fitting stiffness magnitude and phase responses over the frequency range of interest. The elastic, viscous, and inertial parameters computed for the pre-ramp steady-state period were comparable to measures obtained for quasi-static conditions at similar contraction levels, indicating that the time-varying technique was accurate, at least during these intervals. During and immediately following the imposed stretch, however, the fidelity of the model to the observed nonparametric stiffness frequency responses deteriorated significantly, and the model parameters exhibited unexpected variations. The elastic parameter varied in a manner similar to  $K_{low}$  during steady-state periods, but its increase during the ramp stretch itself was usually delayed. The viscous parameter oscillated during the ramp stretch between about 40% and 120% of the pre-stretch value and the inertial parameter unexpectedly doubled during the stretch.

It is possible that these parameter variations reflect important underlying mechanisms; for example, changes in viscosity could be due to rapid changes in crossbridge attachment produced by the imposed stretch, and the apparent increase in joint inertia could be due to an inadequate coupling of the foot to the actuator or to nonlinearities in the stiffness properties. A significant fraction of net viscosity was found to be passive (Fig. 10), however, and the significant decrease in goodness of fit by the second-order model but not by the linear stiffness impulse responses largely rules out poor fixation or nonlinear properties.

It is more likely that these parameter variations arose because the net ankle stiffness dynamics became more complex during the imposed ramp stretch than could be described by the simple second-order model used here. Certainly, the decrease in the %VAF of the second-order fit would support this interpretation, and fitting the wrong parametric model to data is well known to give erratic results (Ljung 1987). Moreover, MacNeil et al. (1992) reported that a second-order ankle stiffness model was also inappropriate during volitional changes in isometric contraction level. We evaluated a simple extension of the second-order model which incorporated a series elasticity to account for tendon compliance. However, this did not significantly improve the fit provided by the second-order model and will therefore not be presented here. It was beyond the scope of the current study to develop a musculoskeletal model capable of describing these results. This is an active research area, however, and improved models capable of predicting the results presented here are anticipated. It should be reiterated, though, that these parameter variations were probably due to an inadequate model of the stiffness frequency responses, not to noise in the frequency responses themselves. The gain cutoff and phase shifts could not be modeled by changes in viscosity and inertia alone, so the unexpected variations in all the model parameters proba-

bly resulted from an inadequate approximation to higher-order (and unmodeled) effects. Furthermore, the fact that the second-order model provides a poor description of system dynamics during the stretch has no effect on the relevance of the nonparametric  $K_{low}$  value; regardless of the changes in system dynamics, this quantity represents the static, elastic component of joint stiffness. The elastic parameter of the second-order model, on the other hand, will almost certainly be distorted by the poor fit of the model to the data during the stretch.

### Stiffness mechanisms

The net ankle torque response to the imposed perturbations (ramp and stochastic) arises from a number of mechanisms, including muscle contractile properties, passive joint properties, and reflex action. The following paragraphs summarize our attempts to characterize the influence of each of these components using changes in task (i.e., active or passive), different stiffness measures (i.e., time-varying, small-amplitude stiffness and steady-state, large-amplitude stiffness), and timing (i.e., before and after reflex latency).

### *Muscle contractile properties*

The time-varying stiffness properties characterized in this study were obtained using a stochastic perturbation with a displacement range of  $\pm 1^\circ$ , which represents less than 2% of the ankle joint range. Length-tension properties are unlikely to make significant contributions to stiffness for such small displacements. However, the small displacement amplitude places the stochastic stiffness responses well within the “short-range” stiffness region (Rack and Westbury 1974; Walmsley and Proske 1981), and the dominance of the torque response to the small stochastic perturbation by the elastic component, coupled with the predominantly nonmuscular origin of the viscous and inertial components, is suggestive of the nearly purely elastic properties of active crossbridges (Julian and Morgan 1981; Zahalak 1986; Lombardi and Piazzesi 1990). We thus believe that  $K_{low}$  (Figs. 5, 7, 8) primarily reflects the intrinsic stiffness of active crossbridges in-series with the muscle tendon. The computation of this quantity with high temporal resolution for an intact human joint is a unique contribution of the time-varying identification technique used in this study.

The behavior of joint torque evoked by the large imposed ramp stretch was rather similar to that described in earlier studies (Allum and Mauritz 1984; Toft et al. 1991), with torque increasing rapidly during the stretch and overshooting slightly before reaching a steady-state value that was significantly larger than the pre-stretch value. The incremental steady-state stiffness typically computed (Fig. 8B) was found to be somewhat smaller in amplitude than  $K_{low}$  obtained using stochastic perturbations, consistent with the view that  $K_{low}$  primarily re-

flects intrinsic “short-range” stiffness properties of active crossbridges, while the incremental stiffness quantity is determined primarily by muscle length-tension properties (i.e., number of available crossbridges) and reflexively mediated changes in muscle activation level.

Yielding, as described for isolated muscle (Joyce et al. 1969; Nichols and Houk 1976; Flitney and Hirst 1978) and intact human joints (Carter et al. 1990), is a rapid decrease in force or torque during an imposed stretch which is presumed to result from the nearly simultaneous disruption of a large fraction of the active crossbridges when their displacement range is exceeded. The amplitude of the ramp stretch used in the current study was much greater in amplitude than the stochastic perturbation and was almost certainly beyond the range where yielding would be expected. The evidence for the presence of yielding in our data is weak, however. The torque response usually exhibited a change in slope during the stretch that coincided with a transient decrease in  $K_{low}$  (Fig. 5), which could indicate the presence of yielding. However, this change in slope coincided with the peak of acceleration, indicating that it probably arose from joint dynamic properties such as inertia rather than from a significant change in elastic stiffness properties. Furthermore, the decrease in  $K_{low}$  during this period was quite brief and followed a transient increase, so that  $K_{low}$  during the stretch never decreased below the pre-stretch level. Indeed,  $K_{low}$  actually increased quite rapidly as the stretch continued – a property that would not be expected in a yielding muscle with a decreased number of attached crossbridges.

Yielding behavior has been described extensively for the cat soleus muscle only (e.g., Joyce et al. 1969; Nichols and Houk 1976), with one study reporting yielding in the human first dorsal interosseus muscle (Carter et al. 1990). Other cat TS muscles either show very subtle yielding effects or none at all (e.g., see Kirsch et al. 1994). Even in the cat soleus muscle, yielding occurs only in an active muscle which is stretched from an initially isometric condition. Deafferented muscle perturbed with a very restricted bandwidth stochastic displacement exhibits no evidence of yielding for perturbation amplitudes at least 3 times the normal range of “short-range stiffness” (Kirsch et al. 1994). The results presented in this current report were also obtained during continuous movement (the small stochastic perturbation), so our failure to observe obvious yielding may result from similar mechanisms. Furthermore, to our knowledge there is no previous evidence of yielding behavior in the human TS muscles. For example, Allum and Mauritz (1984) noted the lack of yielding in their ankle joint responses to dorsiflexing stretches (including ones larger than those used in the current study) and attributed this result to mechanical filtering by connective tissue. We believe that the intact state of the muscles (including inter-muscle connective tissues) and inertial properties due to the mass of the foot may mask or prevent yielding behavior, but differences in the muscle fiber type composition of the human TS muscles relative to the rather unique cat

soleus muscle may also be so significant that yielding would not occur even in the absence of connective tissue. We cannot distinguish between these possibilities from our data, but in either case we believe that yielding, if present at all, is subtle and certainly does not produce the catastrophic effects seen in the cat soleus muscle.

Our estimates of low-frequency stiffness showed that its magnitude actually increased during much of the stretch, even though neural activation remained constant during this interval. This is counter to evidence for yielding behavior in some muscles (as discussed above), but other studies of lengthening muscle have shown similar behavior to that described here. Lombardi and Piazzesi (1990) found that stiffness was always significantly greater during a lengthening stretch than for isometric conditions, even for extremely high stretch velocities. They attributed this enhanced stiffness to either an increase in the excursion range over which crossbridges can remain attached, an increase in the number of attached crossbridges during stretch, or both. A larger range over which attachment can be maintained would result in a larger force generated by a given crossbridge (for a fixed crossbridge stiffness), which in turn would lead to an increase in net muscle stiffness. An increase in the number of attached crossbridges during stretch has also been reported by Julian and Morgan (1979). Lombardi and Piazzesi (1990) hypothesized that this behavior occurs because crossbridges forcibly detached by stretch can reattach 200 times faster than crossbridges which detach after a “normal” contraction cycle.

Our protocol is not directly comparable to that of Lombardi and Piazzesi (1990), however, since they measured stiffness at different constant stretch velocities rather than for a single displacement with a bell-shaped velocity profile. That is, the *dynamics* of stiffness changes were not studied in the isolated muscle fiber. We did study this quantity, but in a whole muscle with many muscle fibers and no control over individual fiber stretch velocities. Even so, the enhanced stiffness during the stretch is consistent with the isolated fiber results of Lombardi and Piazzesi (1990); enhanced muscle fiber stiffness during lengthening (due to either greater force per crossbridge or to a higher number of attached crossbridges) could produce an increase in net muscle stiffness. This increase may be delayed somewhat, perhaps due to some degree of initial “yielding” or to viscous effects in the muscle that we could not accurately estimate.

The maintenance of stiffness ( $K_{low}$ ) after the cessation of lengthening (when muscle fiber properties presumably revert to their lower stiffness “isometric” behavior) must be due to other mechanisms. Changes in the muscle length-tension relationship or in muscle moment arms are not likely mechanisms since the quasi-static stiffness of the ankle showed very little change over the angle range of the stretch (Fig. 6), and passive properties changed only slightly following the large imposed stretch (Fig. 10). It is thus most likely that the steady-state stiffness enhancement seen after the stretch was pri-

marily mediated by the approximately 25% increase in baseline EMG observed during this period.

### *Passive properties*

The passive stiffness properties of the ankle joint were difficult to obtain in isolation due to reflex responses evoked in the TS by the ramp stretch in most subjects, even when they were instructed to relax completely. On the basis of one subject who was able to suppress all reflex action and on the “passive” responses obtained in the other subjects prior to the onset of reflex EMG activity, it appears that passive properties contributed only a modest component to the torque response of the joint and to the net elastic component of joint stiffness. We examined joint properties near the neutral position of the ankle where passive properties are at a minimum, however; stiffness properties for ankle angles near either of the extremes of joint excursion would be expected to contain significantly greater passive components (Weiss et al. 1986a). The viscous component, which accounted for a smaller fraction of the torque variance than the elastic component, contained a large passive component which presumably arose from the viscoelastic properties of the ankle joint capsule and other connective tissue crossing the joint.

### *Reflex action*

The results presented above show that reflex activity evoked by the large imposed stretch was clearly present in both the EMG and torque responses. The superimposed ramp stretch evoked large and repeatable reflex EMG responses in all subjects, followed in most cases by a robust twitch-like torque response. These results are in contrast to those reported by Stein and Kearney (1995), who found that the human ankle reflex torque response to a small position pulse displacement was attenuated progressively as the mean absolute velocity of a superimposed stochastic perturbation increased. For the mean absolute velocity of the stochastic perturbation used in the current study (0.49 rad/s), reflex torque responses would be predicted to be decreased by a factor of 2 to 3 relative to the responses obtained with no superimposed stochastic perturbation. The results presented in Fig. 2 indicate that such severe attenuation was not apparent in the current study, however. We believe that the difference between these studies is due to the higher mean contraction levels used here (12.6–20.3 Nm as compared with the 0–10 Nm range used by Stein and Kearney) and to the use of a maintained stretch 3 times the amplitude of the brief pulse perturbation (akin to a tendon tap) used by Stein and Kearney. It is likely that the stretches in the present experiments were supra-maximal for the stretch reflex and thus overwhelmed any inhibitory effects due to the ongoing stochastic perturbation. We did not examine reflex responses to smaller per-

turbations that may have shown the attenuation predicted by Stein and Kearney.

Even though the effects of reflex activity on several aspects of the joint were clearly present, the time-varying  $K_{low}$  quantity appeared to be independent of both the large burst of ramp stretch-evoked EMG and the twitch-like increase in torque that followed. Likewise,  $K_{low}$  was completely unaffected by the 80–100 ms “silent period” which commenced approximately 60 ms following stretch onset and exhibited an EMG stretch reflex gain of essentially zero (Kirsch and Kearney 1993b). Even though we believe that our current method primarily estimates intrinsic, rather than reflexive, components of stiffness properties, one would expect the intrinsic stiffness to increase in parallel with joint torque following the large ramp-evoked burst of reflex EMG activity. Although this was not observed, it should be noted that in the steady state both stiffness and torque were increased and that the twitch-like reflex contribution to joint torque, although easily observed in most subjects (Fig. 5), was in most cases small in comparison with the overall increase in torque due to the stretch. Thus, a small increase in time-varying stiffness during the reflex twitch may have been too small to detect. It is also possible that the low-frequency stiffness estimate did indeed contain a reflex component that combined with a decrease in intrinsic stiffness to produce a relatively constant net stiffness. We did not examine stretch responses in the absence of reflex action, so further study would be required to assess this and other possible explanations for the lack of an obvious reflex stiffness component.

Although reflex action seemingly produced no obvious change in  $K_{low}$ , the presence of the stochastic perturbation clearly enhanced the torque response to the large imposed ramp stretch. Continuous movement similar to that produced by the stochastic perturbation has previously been found to *reduce* isometric force in isolated muscle preparations (Rack and Westbury 1974; Kirsch et al. 1994), so it is very unlikely that intrinsic muscle mechanisms are responsible for the observed enhancement of the torque response to ramp stretch. It is possible that the perturbation did indeed interfere with muscle contractile mechanisms, requiring the subjects to produce a higher activation level to achieve the required 15% MVC mean ankle torque level. Although baseline EMG levels were significantly larger with the ongoing perturbation than without it (Kirsch and Kearney 1993b), the enhanced torque response to the subsequent ramp stretch indicates that muscle stiffness (which is mediated by the same mechanisms as muscle force) was larger and thus clearly *not* reduced by the stochastic perturbation. The remaining possibility is that the increase in baseline EMG during the perturbation is primarily reflexive in origin and that this particular temporal pattern of activation is somehow more effective in producing muscle stiffness than force.

Whatever the mechanism, the enhancement of the torque response to imposed stretch by the stochastic perturbation suggests that our estimates of time-varying

stiffness magnitude may be larger than would be observed for an unperturbed condition; if so, our conclusions are valid only for the particular experimental conditions tested. It should be noted, however, that stiffness can be measured only by imposing *some* type of perturbation; an ideal input perturbation would provide sufficient excitation to the system under study to evoke all relevant behavior without causing the system to act in an inappropriate or distorted manner. Unfortunately, this ideal is difficult or impossible to attain in a nonlinear system such as the stiffness properties of the intact human ankle joint. We chose a small stochastic perturbation and matched its frequency spectrum to the expected frequency response of ankle stiffness to reduce distortion. Subjects perceived the perturbation as very mild and the torque evoked by it was small compared with the stretch-evoked component. Thus, we believe that the stiffness behavior reported here presents a reasonable picture of the variation in joint stiffness during an imposed movement.

### Implications

The time-varying identification approach described in this study is capable of estimating intrinsic muscle stiffness during nonstationary conditions in a manner not previously possible, and can be used to examine stiffness during other tasks and at other joints. The primary limitation on its applicability is that the selected behavior must be highly repeatable over a large number of repetitions. The behavior examined here is, in many respects, "worst-case" because of the rapid time course of the stretch, but our technique was still able to provide excellent stiffness characterization at 4-ms intervals throughout the stretch.

Several important conclusions resulted from the new information provided by the time-varying stiffness characterization. First, the low-frequency stiffness measure ( $K_{low}$ ) extracted from the identified stiffness impulse responses is likely to be the direct analog of the small amplitude, high frequency stiffness measured in isolated muscle and assumed to be proportional to the number of attached crossbridges (Julian and Morgan 1981; Zahalak 1986; Lombardi and Piazzesi 1990). If so, this quantity uniquely reflects the contractile state of the contracting muscles and can be used during a variety of relevant tasks to examine the muscle properties of an intact system operating in a normal manner. Second, the observed behavior of  $K_{low}$  indicates that muscle "yielding", observed in the cat soleus (Joyce et al. 1969; Nichols and Houk 1976) and in human intrinsic hand muscles (Carter et al. 1990), either was much reduced at the intact human ankle joint or was masked by joint inertia and passive stiffness properties. Furthermore, the increase in stiffness observed during the stretch is consistent with previous results (Lombardi and Piazzesi 1990) in forcibly lengthened isolated muscle fibers. These presumably intrinsic muscle properties indicate that reflex

action may be organized somewhat differently at the intact human ankle joint relative to that of the decerebrate cat TS, where reflex action has been proposed to act primarily to prevent yielding (Nichols and Houk 1976; Hoffer and Andreassen 1981). Third, while a simple second-order model was found to be adequate for describing ankle stiffness dynamics during stationary conditions, it was unable to describe these dynamics accurately during the imposed stretch. A more complex model of joint stiffness is required to describe the nonstationary changes in joint stiffness characterized here and for other tasks which may be examined in a similar manner in the future. Finally, reflex contributions to the time-varying low-frequency stiffness estimated here appear to be small or absent. This may be due to the small magnitude of the reflex component or to its nonlinear nature; indeed, it has been recently shown (Stein and Kearney 1993; Kearney et al. 1994) that a nonlinear identification approach is required to detect such reflex contributions. Further study of the contribution of reflex mechanisms to stiffness properties under a variety of conditions is clearly indicated by the results of this present study.

**Acknowledgements** This work was supported by the Medical Research Council of Canada. RFK was supported by the Cleveland FES Center of the Department of Veterans Affairs PR&D Service during the preparation of this manuscript.

### References

- Allum JHJ, Mauritz K-H (1984) Compensation for intrinsic muscle stiffness by short-latency reflexes in human triceps surae muscles. *J Neurophysiol* 52: 797-818
- Bennett DJ, Hollerbach JM, Xu Y, Hunter IW (1992) Time-varying stiffness of human elbow joint during cyclic voluntary movement. *Exp Brain Res* 88: 433-442
- Bennett DJ (1993a) Torques generated at the human elbow joint in response to constant position errors imposed during voluntary movements. *Exp Brain Res* 95: 488-493
- Bennett DJ (1993b) Stretch reflex responses in the human elbow joint during a voluntary movement. *J Physiol (Lond)* 474: 339-351
- Brown MC, Engberg I, Matthews PBC (1967) The relative sensitivity to vibration of muscle receptors of the cat. *J Physiol (Lond)* 192: 773-800
- Cannon SC, Zahalak GI (1982) The mechanical behavior of active human skeletal muscle in small oscillations. *J Biomech* 15: 111-121
- Carter RR, Crago PE, Keith MW (1990) Stiffness regulation by reflex action in the normal human hand. *J Neurophysiol* 64: 105-118
- Crago PE, Houk JC, Hasan Z (1976) Regulatory actions of human stretch reflex. *J Neurophysiol* 39: 925-935
- Crago PE, Lemay MA, Liu L (1990) External control of limb movements involving environmental interactions. In: Winters JM, Woo SL-Y (eds) *Multiple muscle systems: biomechanics and movement organization*. Springer, Berlin Heidelberg New York, pp 343-359
- Crago PE, Nakai RJ, Chizeck HJ (1991) Feedback regulation of hand grasp opening and contact force during stimulation of paralyzed muscle. *IEEE Trans Biomed Eng* 38: 17-28
- Feldman AG (1966) Functional tuning of the nervous system with control of movement of maintenance of a steady posture III. Mechanographic analysis of the execution by man of the simplest motor tasks. *Biophys USSR* 11: 766-775

- Feldman AG (1974) Change of muscle length due to shift of the equilibrium point of the muscle-load system. *Biofizika* 19: 534–538
- Flitney FW, Hirst DG (1978) Cross-bridge detachment and sarcomere “give” during stretch of active frog’s muscle. *J Physiol (Lond)* 276: 449–465
- Hoffer JA, Andreassen S (1981) Regulation of soleus muscle stiffness in pre-mammillary cats: intrinsic and reflex components. *J Neurophysiol* 45: 267–285
- Hogan N (1985a) Impedance control: an approach to manipulation. I: Theory. II: Implementation. III: Applications. *J Dyn Syst Meas Contr* 107: 1–24
- Hogan N (1985b) The mechanics of multi-joint posture and movement control. *Biol Cybern* 52: 315–331
- Hogan N (1987) Stable execution of contact tasks using impedance control. *Proc IEEE Conf on robotics and automation*, pp 1047–1054
- Hunter IW, Kearney RE (1982) Dynamics of human ankle stiffness: variation with mean ankle torque. *J Biomech* 15: 747–752
- Jack JJB (1978) Some methods for selective activation of muscle afferent fibres. In: Porter R (ed) *Studies in neurophysiology*. Cambridge University Press, Cambridge, pp 157–176
- Joyce GC, Rack PMH, Westbury DR (1969) The mechanical properties of cat soleus muscle during controlled lengthening and shortening movements. *J Physiol (Lond)* 204: 461–474
- Julian FJ, Morgan DL (1979) The effect on tension of non-uniform distribution of length changes applied to frog muscle fibres. *J Physiol (Lond)* 293: 379–392
- Julian FJ, Morgan DL (1981) Tension, stiffness, unloaded shortening speed and potentiation of frog muscle fibres at sarcomere lengths below optimum. *J Physiol (Lond)* 319: 205–217
- Kearney RE, Kirsch RF, MacNeil JB, Hunter IW (1991) An ensemble time-varying identification technique: theory and biomedical applications. *International Federation of Automatic Control Symp on identification and system parameter estimation*, pp 191–195
- Kearney RE, Stein RB, Parmeswaran L (1994) Differential identification of passive and reflex mechanisms in human ankle stiffness dynamics. *16th Ann Int Conf IEEE Engineering in Medicine and Biology Society*
- Kearney RE, Hunter IW (1982) Dynamics of human ankle stiffness: variation with displacement amplitude. *J Biomech* 15: 753–756
- Kirsch RF, Kearney RE (1991) Time-varying identification of human ankle joint stiffness dynamics during imposed movement. *13th Ann Int Conf IEEE Engineering in Medicine and Biology Society*, pp 2030–2031
- Kirsch RF, Rymer WZ (1992) Neural compensation for fatigue induced changes in muscle stiffness during perturbations of elbow angle in man. *J Neurophysiol* 68: 449–470
- Kirsch RF, Kearney RE (1993a) Identification of time-varying human ankle joint stiffness produced by an imposed stretch. *Proc 19th Canadian medical and biological engineering conference*, pp 316–317
- Kirsch RF, Kearney RE (1993b) Identification of time-varying dynamics of the human triceps surae stretch reflex. II. Rapid imposed movement. *Exp Brain Res* 97: 128–138
- Kirsch RF, Kearney RE, MacNeil JB (1993) Identification of time-varying dynamics of the human triceps surae stretch reflex. I. Rapid isometric contraction. *Exp Brain Res* 97: 115–127
- Kirsch RF, Boskov D, Rymer WZ (1994) Muscle stiffness during transient and continuous movements of cat muscle: perturbation characteristics and physiological relevance. *IEEE Trans Biomed Eng* 41: 758–770
- Lacquaniti F, Carrozzo M, Borghese NA (1993) Time-varying mechanical behavior of multijointed arm in man. *J Neurophysiol* 69: 1443–1464
- Lan N, Crago PE, Chizeck HJ (1991) Control of end-point forces of a multijoint limb by function neuromuscular stimulation. *IEEE Trans Biomed Eng* 38: 953–965
- Latash ML, Gottlieb GL (1991a) Reconstruction of shifting elbow joint compliant characteristics during fast and slow movements. *Neuroscience* 43: 697–712
- Latash ML, Gottlieb GL (1991b) Virtual trajectories of single-joint movements performed under two basic strategies. *Neuroscience* 47: 357–365
- Latash ML (1992) Virtual trajectories, joint stiffness, and changes in the limb natural frequency during single-joint oscillatory movements. *Neuroscience* 49: 209–220
- Ljung L (1987) *System identification: theory for the user*. Prentice-Hall, Englewood Cliffs, NJ
- Lombardi V, Piazzesi G (1990) The contractile response during steady lengthening of stimulated frog muscle fibres. *J Physiol (Lond)* 431: 141–171
- MacNeil JB, Kearney RE, Hunter IW (1992) Identification of time-varying biological systems from ensemble data. *IEEE Trans Biomed Eng* 39: 1213–1225
- Nichols TR, Houk JC (1976) Improvement in linearity and regulation of stiffness that results from actions of stretch reflex. *J Neurophysiol* 29: 119–142
- Rack PMH, Westbury DR (1974) The short range stiffness of active mammalian muscle and its effect on mechanical properties. *J Physiol (Lond)* 240: 331–350
- Salisbury JK (1980) Active stiffness control of a manipulator in Cartesian coordinates. *19th IEEE Conf on decision and control*, pp 95–100
- Stein RB, Kearney RE (1993) Nonlinear behavior of stretch reflexes at the human ankle joint. *15th Ann Int Conf IEEE Engineering in Medicine and Biology Society*, pp 1167–1168
- Stein RB, Kearney RE (1995) Nonlinear behavior of muscle reflexes at the human ankle joint. *J Neurophysiol* 73: 65–72
- Toft E, Sinkjaer T, Andreassen S, Larsen K (1991) Mechanical and electromyographic responses to stretch of the human ankle extensors. *J Neurophysiol* 65: 1402–1410
- Walmsley B, Proske U (1981) Comparison of stiffness of soleus and medial gastrocnemius muscles in cats. *J Neurophysiol* 46: 250–259
- Weiss PL, Kearney RE, Hunter IW (1986a) Position dependence of ankle joint dynamics. I. Passive mechanics. *J Biomech* 9: 727–735
- Weiss PL, Kearney RE, Hunter IW (1986b) Position dependence of ankle joint dynamics. II. Active mechanics. *J Biomech* 9: 737–751
- Weiss PL, Kearney RE, Hunter IW (1988) Human ankle joint stiffness over the full range of muscle activation levels. *J Biomech* 21: 539–544
- Zahalak GI (1986) A comparison of the mechanical behavior of the cat soleus muscle with a distribution-moment model. *J Biomech Eng* 108: 131–140